DOI: 10.1002/chem.200601108

First-Principles Molecular Dynamics Evaluation of Thermal Effects on the NMR $^{1}J_{Li,C}$ Spin–Spin Coupling

Aurélien de la Lande,[a] Catherine Fressigné,[b] Hélène Gérard,[a] Jacques Maddaluno,[b] and Olivier Parisel*[a]

Abstract: Car–Parrinello (CP) molecular dynamics were applied to sample conformations of various models of organolithium aggregates which are chosen to estimate $^{1}J_{Li,C}$ NMR coupling constants. The results show that the deviations from the values computed using static (optimized) geometries are small provided no large-amplitude motions occur within the timescale of the simulations. In the case of the vinyllithium dimer, for which rotation of the vinyl chain is observed, this approach allows analysis of the various contributions to the experimentally measured constants. For the trisolvated methyllithium monomer, partial decoordination of solvating dimethyl ether is observed and results in a significant shift of $^{1}J_{Li,C}$. All these results highlight that a varied physicochemical machinery is hidden behind general empirical formulas, such as the Bauer–Winchester–Schleyer rule used experimentally.

Keywords: aggregation · lithium · molecular dynamics · NMR spectroscopy · solvation

Introduction

Alkyl lithium compounds are widely used reagents in organic synthesis.[1] Their structure in solution exerts a dramatic influence on reactivity and stereoselectivity, especially due to aggregation and solvation processes.[2–6] Characterization of the structural arrangements of such polar organometallics in solution is now generally performed by using NMR spectroscopy, which affords convenient access to important physicochemical characteristics.[7–9] In particular, the $^{1}J_{Li,C}$ coupling constant is a useful parameter which can be directly related to the degree of aggregation of the organolithium compound, independent of the nature of the organic chain. Indeed Bauer, Winchester, and Schleyer have proposed an empirical formula [BWS rule; Eq. (1)]

$$^{1}J_{Li,C}\ [\mathrm{Hz}] = (17 \pm 2)/n \qquad (1)$$

where n is the number of carbon atoms directly linked to the lithium atom.[10] This rule applies to the determination of the degree of aggregation from experimental data and to the prediction of coupling constants in homogeneous or heterogeneous organolithium aggregates. From a computational point of view, reproduction of this rule has been undertaken to both better understand its origin and ensure it also applies to species undetectable by NMR yet. It was shown, in particular for monomeric species, that the inclusion of explicit solvent molecules and electronic correlation is essential to reach proper agreement.[11,12]

Further improvement in the description of organolithium compounds should thus take both aggregation and solvation into account. This is roughly achieved by means of quantum-chemical computations, since these processes are associative/dissociative phenomena for which entropic contributions play an important role: the internal energy is not sufficient to describe the chemical equilibrium. We have recently shown that the free energies can be computed either by evaluating entropic variations using vibrational frequencies within the harmonic approximation coupled to an appropriate statistical treatment, or by using molecular dynamics simulations.[13] Note that, in the latter case, quantum effects on the nuclei (zero-point energy corrections) can only be included if an adapted procedure such as a path integral treatment is used, the cost of which is much higher than classical Car–Parrinello (CP) ab initio molecular dynamics (AIMD).[14] To our knowledge, the only current approaches

[a] Ing. A. de la Lande, Dr. H. Gérard, Dr. O. Parisel
Laboratoire de Chimie Théorique, UMR 7616 CNRS
Université P. & M. Curie, Case Courrier 137
4, place Jussieu, 75252 Paris Cedex 05 (France)
Fax: (+33) 144-274-117
E-mail: olivier.parisel@lct.jussieu.fr

[b] Dr. C. Fressigné, Dr. J. Maddaluno
Laboratoire des Fonctions Azotées &
Oxygénées Complexes de l'IRCOF, UMR 6014 CNRS
Université de Rouen, 76821 Mont-Saint-Aignan Cedex (France)

resort to an average of values associated with a series of thermally sampled structures[15] or to normal-mode expansions of the property investigated.[16]

However, such a methodology is not straightforward, since for each newly studied compound the number of coordinated solvent molecules and the preferred degree of aggregation cannot be easily predicted from computations.[17–19] The prediction is especially difficult due to the small energy gaps between the different possible degrees of solvation and aggregation. These can be easily overcome by entropic effects, which are poorly rendered by static computations. In contrast, quantum dynamics calculations can give access to "time-optimized" species provided the energy barriers between the various interconverting entities remain reasonably low. This prompted us to evaluate the performance of these methods in describing the geometrical and energy parameters of model organolithium aggregates.[13] However these primary structural data are hardly accessible from experiments in solution. We thus thought it could be insightful to compare NMR coupling constants, computed on the basis of ab initio molecular dynamics, to available experimental or extrapolated data. Overall, the goal of this article is thus to evaluate the effects of thermal motion on computed coupling constants.

Before discussing these points further, we emphasize that the well-known dynamic behavior of alkyl lithium species observed by NMR spectroscopy[7] cannot be reproduced from molecular dynamics simulations: the timescale of Car–Parrinello simulations[20] is about 10^6 times shorter than that of NMR spectroscopy. Consequently, the computed thermally averaged results should not be mistaken with the dynamic behavior of aggregates as recovered from NMR experiments, which mostly consists of internal rearrangements. In the latter case, a simple average of the coupling constants computed for each "static" local minimum can provide the desired information.[4b] An obvious example is the static versus fluxional behavior of the MeLi tetramer. In this cubic structure, at low temperature, each lithium atom is surrounded by three carbon atoms. The three corresponding coupling constants are thus given by inserting $n=3$ in Equation (1), that is $^1J_{Li,C}=17/3=5.7$ Hz. The fourth Li–C coupling is associated with a long diagonal of the cube and thus exhibits a quasizero coupling constant.

At temperatures that reveal the presence of fluxional species, the NMR acquisition timescale can be regarded as long with respect to exchange between isotopomers. Four arrangements around a single lithium cation are thus necessary to account for the experimental data (Figure 1). In consequence, the observed coupling constant is the average of the coupling constants of the four structures. For instance, the coupling between Li and C^1 is 17/3 for the three first structures and 0 for the fourth, and hence we obtain Equation (2).

$$^1J_{Li,C}(\text{flux})=\frac{1}{4}\left[3\times\left(\frac{17}{3}\right)+1\times 0\right]=\frac{17}{4}=4.3\text{ Hz} \qquad (2)$$

Therefore, the fourfold coordination suggested by the BWS rule in such a case can be proposed to result from averaging over four structures, each of which has three C–Li bonds. Reproducing the BWS value thus does not require any thermal motions around the equilibrium, but elementary statistical considerations.

On the other hand, the CP timescale remains very small with respect to that of isotopomerization; consequently, no such process is observed within the simulation time.[13] Exchange between minima will only occur if the energy barrier is small enough. The motions sampled in such simulations are thus to be considered as fluctuations around one of the local minima. The thermal effects on the $^1J_{Li,C}$ coupling constants reported here thus result from the influence of these fluctuations on the computed values and are not to be compared to the "fluxional" NMR data obtained at sufficiently high experimental temperature. They are to be considered as complementary information to the "static" features.

The general procedure designed for this study consisted of the preliminary validation of the influence of the computational level on the $^1J_{Li,C}$ constants by using structures sampled from the CP simulations. Next, the monomeric, dimeric, and tetrameric structures of unsolvated MeLi were used as benchmarks to evaluate the improvements brought by a thermal treatment. Note that this step also allows better understanding of the chemical roots of the empirical BWS rule. A thermally averaged description of the coupling constants in the aggregates was deduced. This approach was then applied to the case of vinyllithium dimers, for which the $^1J_{Li,C}$ coupling constants exhibit strong dependence on the conformation of the vinyl moieties. Finally, explicit microsolvation was included for the monomer. Taken together, our results delineate the scope of both the static and the dynamic approaches for the treatment of organometallics in solution and highlight the phenomenological aspects justifying the empirical BWS rule.

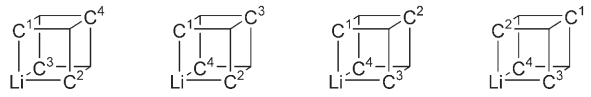

Figure 1. Four possible arrangements of four C atoms around one Li atom, corresponding to four equivalent isotopomers of the MeLi tetramer.

Computational Details

The geometry optimizations and the NMR coupling constant computations[21] were carried out using the Gaussian 03 program.[22] The basis set and the DFT methods used for NMR evaluations are detailed in the text. For CP calculations, the PINY-MD program was chosen,[23] using the BLYP functional,[24] a plane-wave (PW) basis set, and Goedecker (Li)[25] and Trouiller–Martins (other atoms)[26] pseudopotentials; this approach is hereafter referred to as BLYP/PW. We employed the cluster boundary condition method by Martyna and Tuckerman[27] but a dual-box formalism[28] in the case of solvated systems. The plane-wave energy cut-off E_{cut} was 80 Rydberg.[14a] Both E_{cut} and the box size were adjusted for each

system to yield energies converged to chemical accuracy.[13] CP simulations were carried out using optimized BLYP/6-31+G** structures as starting points. A constant temperature (300 K) was ensured thanks to Nosé–Hoover chains of length 4 on the atoms.[29] It was checked that the fictitious electron kinetic energy remained small compared to that of the nuclei (adiabadicity) without need for electronic thermostating. A fictitious mass of 650 amu was used. In all simulations, the time step was set to 0.125 fs. The total simulation time was about 10 ps for each species investigated.

Validation of the Computational Level for Computing Coupling Constants

Taking electronic correlation into account: In our previous paper,[11] only HF and MP2 values were computed, due to software limitations. It was concluded that electronic correlation had to be taken into account to quantitatively reproduce the impact of aggregation. Since DFT evaluation of coupling constants was recently made available,[22] at much more reasonable cost than MP2 computations, we extended our original results to various available functionals[24,30,31] using the same protocol (B3P86/6-31G** optimized geometry, and 6-31G** basis set for NMR) and set of molecules (Table 1). In general, the calculated $^1J_{Li,C}$ are larger than the experimental estimates, except for the solvated monomer. Overall, the MP2 values remain the closest to the BWS empirical estimates, but the much cheaper hybrid functionals (B3P86 and PBE1PBE) are reasonably similar. A larger deviation is obtained with the nonhybrid functionals (BLYP and PBEPBE). Nevertheless, the magnitude and order of the differences are not systematic, so further investigations into the factors influencing the quality of the results were undertaken.

Table 1. $^1J_{Li,C}$ coupling constants [Hz] computed for MeLi aggregates and solvated monomers. Geometries were optimized at the B3P86/6-31G** level.

	MeLi	$(MeLi)_2$	$(MeLi)_4$	$MeLi(Me_2O)_3$
BWS values	17[a]	8.5	5.7	17[a]
HF/6-31G**	41.0	11.7	7.0	14.6
MP2/6-31G**	25.9	9.9	6.0	–
B3P86/6-31G**	27.6	10.6	7.0	15.5
BLYP/6-31G**	35.9	11.4	7.4	18.0
PBEPBE/6-31G**	35.9	11.3	7.4	17.9
PBE1PBE/6-31G**	31.9	10.9	7.0	15.9

[a] Value computed using the degree of aggregation only.

Choice of basis set: It was shown previously[13] that BLYP/PW energies and geometries are of similar accuracy to those obtained with a Gaussian basis set, provided the latter is of very high quality, namely, 6-311++G(2d,2p). Nevertheless, for a given geometry, it is still necessary to find out what kind of basis set should be used to obtain reliable coupling constants. All $J_{Li,C}$ coupling constants for LiMe aggregates were computed with various basis sets. Since it was also established that BLYP and B3P86 yield similar energetical data provided the same basis is used, the constants were all computed using the BLYP/6-311++G(2d,2p) optimized geometries. Results are given in Table 2. The $^1J_{Li,C}$ coupling constants were obtained for the monomer, the dimer and the tetramer. An additional set of $^3J_{Li,C}$ constants, corresponding to atoms located across the cube, was also computed but, as they are too small to be detected experimentally and were indeed found to be close to zero from computations, whatever the basis set, they are not studied any further in this paper. Several different $^1J_{Li,C}$ coupling constants were obtained for each dimer or tetramer due to the conformational behavior of the methyl group. Therefore, an averaged value within a given structure is reported (Table 2), together with the amplitude of the variation.

Table 2. $^1J_{Li,C}$ and $^3J_{Li,C}$ coupling constants [Hz] computed using the BLYP functional for $(LiMe)_4$ (cubic), $(LiMe)_2$, and (LiMe) with various basis sets and geometries optimized at the BLYP/6-311++G(2d,2p) level.

	Tetramer				Dimer		Monomer[c]
	$^1J_{Li,C}$		$^3J_{Li,C}$		$^1J_{Li,C}$		$^1J_{Li,C}$
	Average[a]	Max−Min[b]	Average[a]	Max−Min[b]	Average[a]	Max−Min[b]	Value
6-31G**	7.50	0.19	0.403	0.004	11.58	1.29	35.92
6-31+G**	7.93	0.22	0.404	0.006	10.67	1.01	31.81
6-311+G**	8.38	0.28	0.129	0.002	12.82	1.66	39.74
6-311++G(2d,2p)	8.42	0.29	0.140	0.003	12.93	1.48	39.53

[a] Average of all the $^1J_{Li,C}$ coupling constants in a given structure. [b] Difference between the largest and the smallest $^1J_{Li,C}$ values in a given structure. [c] 6-311++G(3df,3dp): 39.73 Hz; cc-pCVQZ: 41.77 Hz; aug-cc-pCVQZ: 41.53 Hz; cc-pVQZ: 41.75 Hz; cc-pVTZ: 40.15 Hz.

Absolute values for $^1J_{Li,C}$ are found to depend significantly on the basis set, whatever the degree of aggregation, as variations of up to 20% are obtained between the constants from the smallest basis set (6-31G**) and those from the reference basis set, namely, 6-311++G(2d,2p). Since convergence with the basis set size is reached for the 6-311+G** basis, the key feature allowing a reliable computation of the coupling constants thus appears to be the use of a triple-ζ basis set. It is probably required to recover a proper description of the electron density between the carbon and lithium atoms and improved energy location of the virtual orbitals, two features out of reach for the less flexible double-ζ basis. Consequently, 6-311+G** is the smallest basis set that can be used, and it was thus retained for the remainder of this study.

Choice of functional: The $^1J_{Li,C}$ coupling constants were next computed for various functionals and degrees of aggregation for BLYP/6-311++G(2d,2p) optimized geometries. The results are given in Table 3. In contrast to the results of Table 1, the 6-311+G** basis set yields similar results for the hybrid PBE1PBE and nonhybrid PBEPBE functionals. On the other hand, the BLYP values are systematically over-

Table 3. Computed $^1J_{Li,C}$ coupling constants [Hz] for aggregates of methyllithium (BLYP/6-311++G(2d,2p) optimized geometries except for $(MeLi)(OMe_2)_3$, for which BLYP/6-31++G** was used) with the 6-311+G** basis set.

	MeLi	$(MeLi)_2$	$(MeLi)_4$	$MeLi(OMe_2)_3$
BWS values	17.0 ± 2[a]	8.5 ± 1	5.6 ± 0.7	17.0 ± 2[a]
BLYP/6-311+G**	39.74	12.83	8.38	18.76
PBEPBE/6-311+G**	35.19	11.28	7.29	17.24
PBE1PBE/6-311+G**	35.89	11.64	7.45	17.75

[a] Value computed using the degree of aggregation only.

estimated by more than 1 Hz. PBEPBE was finally retained since this nonhybrid functional consumes much less CPU time and thus allows bulk evaluation of coupling constants.

To get a better insight into the origin of the discrepancy between BLYP and PBEPBE coupling constants, both bases were applied to unoptimized structures extracted from the CP simulation on the monomer, the dimer, the tetramer, and the solvated monomer. These four systems cover a large range of $^1J_{Li,C}$ values and thus allow conclusions to be drawn for any degree of aggregation or solvation. The PBEPBE values were found to be simply correlated to the BLYP values by the linear regression $^1J_{Li,C}(PBEPBE) = 0.8897\,^1J_{Li,C}(BLYP) - 0.1388$. A very good correlation coefficient was obtained ($R^2 = 0.9995$). The differences between PBEPBE and BLYP in Table 3 are thus systematic and can be corrected by using this regression if desired.

Evaluation of dynamic effects on the coupling constants: Thermal effects on $^1J_{Li,C}$ were evaluated by a posteriori computation of the $^1J_{Li,C}$ values on geometries sampled from a constant-temperature CP simulation. A further statistical treatment was then carried out on the extracted constants by averaging, computing root-mean-square deviations (RMSDs), and plotting probability distribution functions. To examine the number of snapshots required for this statistic to be meaningful, $^1J_{LiC}$ were averaged for one couple of LiC atoms in the dimer over an increasing number of points (Figure 2). It was found that the $^1J_{LiC}$ value converges toward an experimentally relevant accuracy of 0.1 Hz within less than 300 snapshots for a simulation time of 15 ps, which corresponds to a snapshot taken every 50 fs. This value was retained for the other systems considered in this contribution.

The procedure for evaluating $^1J_{Li,C}$ thus consists of the following steps:

1) Optimize the structure of the desired species and compute the static coupling constant at the BLYP/6-311+G** level.
2) Carry out a constant-temperature CP simulation using this optimized structure as a starting point.
3) Sample the simulation for geometries at a time period smaller than 50 fs and compute the coupling constant for each snapshot at the BLYP/6-311+G** level.
4) Collect and analyze the obtained coupling constants.

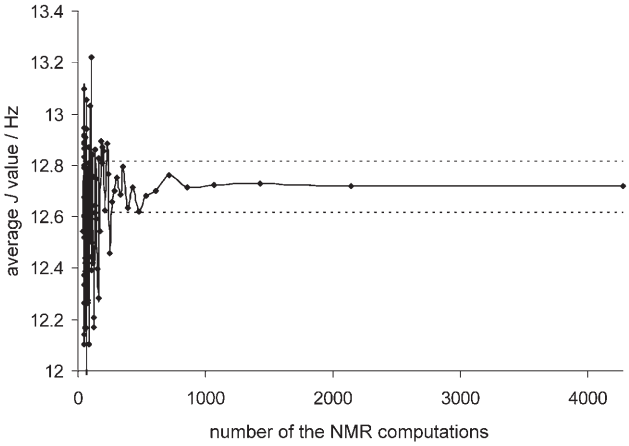

Figure 2. $^1J_{Li,C}$ (BLYP/6-311+G**) averaged over an increasing number of equally spaced CP computation snapshots (BLYP/PW). The dotted lines represent the averaged value $\pm$ 0.1 Hz.

Results and Discussion

We first applied our procedure to the monomer, dimer, and tetramer of MeLi, for which the static NMR coupling constants[11] (step 1) and the geometrical behavior around the optimum geometry[13] (step 2) have already been described elsewhere. Effects of large amplitude motions or discrete solvation were then examined by applying the entire scheme to the dimer of vinyllithium and to the trisolvated monomer $MeLi(OMe_2)_3$.

Effect of aggregation: The coupling constants for the monomer, dimer, and tetramer of MeLi were computed according to step 3 of the procedure. The corresponding distribution functions are plotted in Figure 3. The averaged values and corresponding RMSDs are given in Table 4. Additionally, parameters for both the planar and cubic structures of the tetramer were computed. Indeed, structural consequences of thermal fluctuations were shown to be very different for these two isomers of the tetramer.[13] We thought it could be

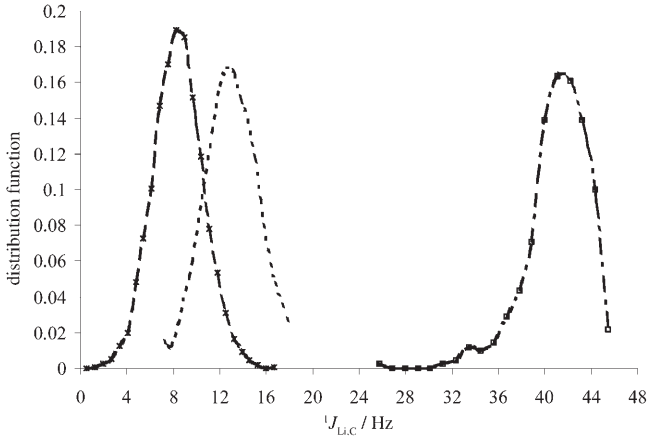

Figure 3. $^1J_{Li,C}$ (BLYP/6-311+G**) distribution function for the monomer (–•–•), dimer (-----), and tetramer (–––) of MeLi.

Table 4. BWS, static, and 300 K averages and RMSDs for $^1J_{Li,C}$. Average over all equivalent constants is given. Static values were computed using the 6-311++G(2d,2p) basis.

		MeLi	$(MeLi)_2$	$(MeLi)_4$, cubic	$(MeLi)_4$, planar
$^1J_{Li,C}$ [Hz]	BWS	17.0	8.5	5.7	8.5
	static	39.7[a]	12.8	8.4	15.1
	average	40.6	12.8	8.0	14.8
	RMSD	2.7	2.4	2.2	2.00
Li–C	static	1.98	2.11	2.20	2.06
distance	average	1.99	2.12	2.23	2.08
[Å]	RMSD	0.07	0.10	0.13	0.09

[a] This value can be decomposed as follows: Fermi contact: 39.91 Hz; spin–dipolar: −0.10 Hz; paramagnetic spin–orbit: −0.09 Hz; diamagnetic spin–orbit: 0.02 Hz.

an efficient system to evaluate thermal effects on $^1J_{Li,C}$ values.

The averaged and optimized values for the computed $^1J_{Li,C}$ coupling constants compare remarkably well (Table 4). It is especially noteworthy that no major effect is observed for the planar structure of the tetramer, for which geometrical fluctuations were found to be quite large.[13] Consequently, the agreement with the values predicted by the BWS rule is not improved by dynamical averaging. On the other hand, the RMSD was found to be insensitive to the degree of aggregation (and thus to the value of $^1J_{Li,C}$) and to be quite large (ca. 2.5 Hz, about ten times the experimental accuracy). Still, no special behavior of the planar structure is observed, despite its greater flexibility. The similarity between the $^1J_{Li,C}$ value obtained from static geometry optimization and that using the above-mentioned sampling procedure is worth noting since this agreement is the consequence of the averaging of widely scattered data. For example, $^1J_{Li,C}$ for the tetramer briefly reaches values close to zero, and thus equal to that of the $^3J_{Li,C}$ constant. This behavior should, however, not be mistaken with exchange between proximal and distal C atoms at a given Li atom nor with significant lengthening of the Li–C bond. As pointed out previously,[13] no such topomerization or distortion of the structure is observed within the simulation time.

The evolution of the coupling constants with the degree of aggregation suggests that the values of $^1J_{Li,C}$ decrease as the coordination number at the Li cation increases. In comparison, the variations in RMSDs are much smaller and hardly significant (Figure 3).

A correlation between the evolution of $^1J_{Li,C}$ and that of the Li–C distances is both tempting and frustrating. Intuitively, the longer Li–C bonds correspond to smaller coupling constants (Table 4), whereas, overall, widely scattered values of the Li–C distances do not correspond to a larger RMSD for the corresponding $^1J_{Li,C}$ coupling constant. We thus tried to correlate $^1J_{Li,C}$ to some other geometrical parameters (Figure 4) for the simple case of monomeric MeLi. $^1J_{Li,C}$ did not correlate to the Li–C distance. No better result was obtained when using the shortest Li–H distance. The best fit was obtained for the sum of the three H-C-Li angles Σ_θ, which allows evaluation of the pyramidalization at the carbon center and thus estimation of the hybridization and the weight of s character in the axial hybrid. The linear regression of $^1J_{Li,C}$ with $\cos(\Sigma_\theta)$ yields a correlation coefficient of 0.75. More than 75% of the points are located between two threshold curves (shown in Figure 4, bottom), given by Equations (3) and (4).

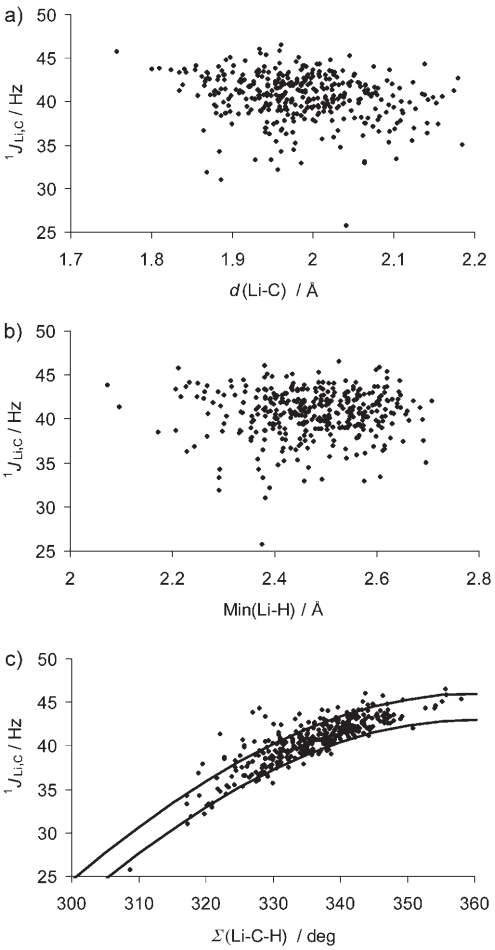

Figure 4. $^1J_{Li,C}$ (BLYP/6-311+G**) as a function of the Li–C distance (a), the shortest Li–H distance (b) and the sum of the Li-C-H angles (c).

$$J\ [\mathrm{Hz}] = 43.0\cos(\Sigma_\theta) + 0.0 \quad (3)$$

$$J\ [\mathrm{Hz}] = 43.0\cos(\Sigma_\theta) + 3.0 \quad (4)$$

This Karplus-like relationship[32] is perfectly in line with the commonly admitted guidelines for ^1J constants when governed by the Fermi-contact contribution, as is the case here (Table 4): the greater the s character of the involved hybrids, the larger the coupling.[33] Indeed, a value of zero would be found for $\Sigma_\theta = 270°$ from Equation (3), which corresponds to a limiting situation with three Li-C-H angles of 90°, as would be the case in a planar carbanion interacting with a Li^+ ion (i.e., a purely p Li–C bonding scheme). When the angles increase, the s character of the Li–C bonding increases and so does the coupling constant.

In conclusion, this study shows that the large number of points used to evaluate the averaged $^1J_{Li,C}$ value allows better understanding of the impact of fundamental geometrical parameters on statically computed coupling constants. Whereas $^1J_{Li,C}$ can be obtained from optimized structures, RMSDs could neither be calculated nor analyzed by using a static approach. Even though taking thermal effects into account does not improve the fit between the DFT and BWS evaluations of the $^1J_{Li,C}$ coupling constants, these effects are of significant amplitude. This validates the approach used in this study, which consists of averaging widely scattered microscopic NMR data to yield macroscopic $^1J_{Li,C}$ coupling constants. This proves to be especially valuable in the case of systems exhibiting multiple minima, as will be shown in the following example.

Table 5. Static and 300 K averages and RMSDs for $^1J_{Li,C}$ in the vinyllithium dimers. Static structures were optimized at the BLYP/6-311++G(2d,2p) level.

Relative energies	*ortho-syn* 0.00 kcal mol^{-1}	*ortho-anti* 0.54 kcal mol^{-1}	*para* 0.11 kcal mol^{-1}
Li–C$_\alpha$ [Å]	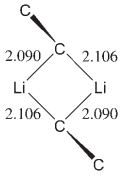	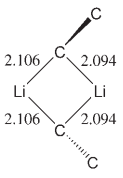	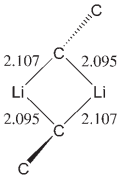
$^1J_{Li,C}$ [Hz]	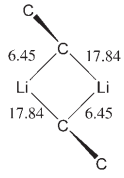	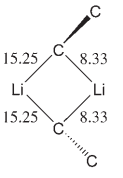	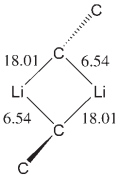
	average = 12.15	average = 11.79	average = 12.28
Time-averaged distances [Å]		*d*(Li–C) RMSD	
	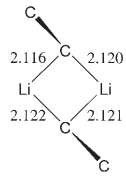 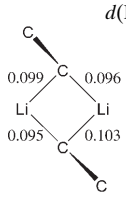		
	Average over the four Li–C distances: 2.120 (RMSD = 0.098)		
Time-averaged $^1J_{Li,C}$ [Hz]		$^1J_{Li,C}$ RMSD	
	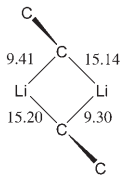 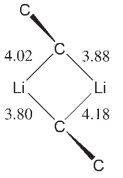		
	Average over the four Li–C coupling constants: 12.26 (RMSD = 4.92)		

Modeling large-amplitude motions: The unsolvated vinyllithium dimer provides a prototype example for a species exhibiting rapidly interconverting multiple minima at low temperature. The computational evaluation of the $^1J_{Li,C}$ coupling constant for the monomer was first investigated by Ruud et al. using various correlated methods.[34] For the dimer, three minima, shown in Figure 5, are found within 0.6 kcal mol^{-1} (Table 5). They are characterized by the relative *syn* or *anti* conformation of the vinyl moieties, either with respect to one another or with respect to the Li–Li axis.

Figure 5. Three lower energy conformations for the vinyllithium dimer: *ortho-syn* (left), *ortho-anti* (center), and *para* (right).

The $^1J_{Li,C}$ coupling constants are highly dependent on the conformation of the vinyl moieties, as evidenced by the schematic representations provided in Table 5. For a given α-carbon atom, two very different coupling constants are computed: a "small" one corresponding to the Li atom close to the C$_\beta$ atom of the same vinyl group, and a "large" one corresponding to the other Li atom. These two values differ by about 10 Hz. Assuming fast rotation of the vinyl moiety with respect to the NMR timescale leads to a single $^1J_{Li,C}$ experimental coupling constant.[35] Such an averaging can be obtained, as proposed in the introduction, by averaging the four $^1J_{Li,C}$ constants. The computed constants (ca. 12 Hz), averaged over these two values, are reasonably larger than those predicted from the BWS value (which is known to remain valid for sp^2-hybridized species[7]) for the dimers (ca. 8 Hz), but are slightly smaller than those obtained for the MeLi dimer (12.8 Hz), in which no large-amplitude motion occurs.

A dynamic study was undertaken to evaluate the possibility of thermal exchanges between the three structures. The orientation of the vinyl moieties with respect to the Li–Li axis or to one another are reported in Figure 6 (top). Numerous exchanges between configurationally stable structures are observed. The preferred orientation of one vinyl

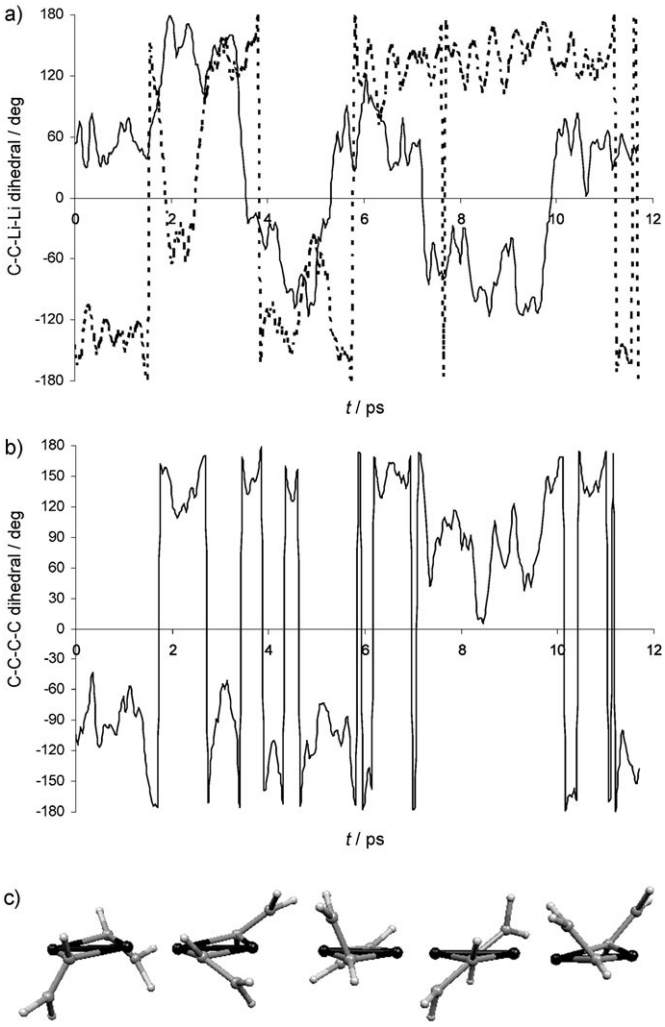

Figure 6. Orientation of the vinyl moieties with respect to the Li–Li axis (a) and with respect to one another (b). c) snapshots at $t=1$, 3, 5, 7, and 8 ps.

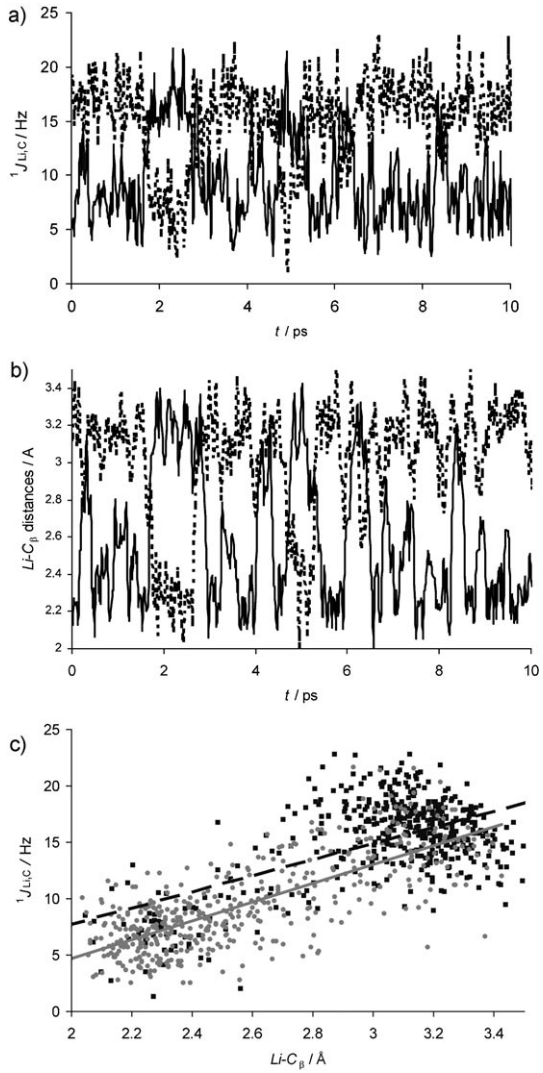

Figure 7. a) $^1J_{Li,C}$ coupling constants for one of the α-carbon atoms and b) the corresponding Li–C_β distance as a function of time in the dimer of vinyllithium. c) A correlation between these two values is plotted.

moiety with respect to the Li–Li axis is either ±60° or ±120°, whereas orientations at ±60°, ±120°, and 180° are found for one vinyl group with respect to the other. This corresponds to fast interconversion between all three minima shown in Figure 5, as evidenced by the snapshots in Figure 6 (bottom). The Li–C_α distance averaged along the simulation is about 0.02 Å longer than that obtained from static computations. This difference is hardly meaningful since it is of the same order of magnitude as the corresponding RMSD.

Using the procedure described above, the four $^1J_{Li,C}$ coupling constants were computed along the simulation. Two of them, for one given carbon atom, are given in Figure 7. Numerous exchanges between small and large values of $^1J_{Li,C}$ are found, consistent with the numerous rearrangements occurring between the various conformers described above. Nevertheless, as pointed out in the introduction, the full averaging of the molecular motions observed in NMR experiments cannot be obtained from CP simulations. This results in an overestimated representation of the starting structure with respect to the other conformers (Table 5). In particular, all symmetric counterparts should be as abundant, so that, as for the static results, a value reproducing the NMR data can be obtained by averaging the four $^1J_{Li,C\alpha}$ constants. Under these conditions, the resulting value is similar to the average of the four static constants.

The coupling constants for the dimers of methyl- and vinyllithium were found to be almost identical, as commonly accepted. Nevertheless, such similar values result from highly different behaviors, as reflected, for example, in the RMSDs. It is thus remarkable that, despite the sensitivity of $^1J_{Li,C}$ to microscopic factors such as, among others, aggregation number, geometrical characteristics, thermal or electronic effects, the simple BWS rule remains so efficient. This observation suggests that structural and dynamic data are still hidden behind averaging. Microscopic simulations could

hopefully inspire new NMR sequences that would allow them to be extracted from experiments.

Effect of solvation: Since explicit representation of solvation was shown to be essential for proper evaluation of coupling constants, the impact of thermal fluctuations on this parameter was next evaluated for the CH_3Li monomer by means of a CP molecular dynamics simulation on the trisolvated species $CH_3Li(OMe_2)_3$. Dimethyl ether was chosen as the smallest model for the ethereal solvents commonly used experimentally. The $^1J_{Li,C}$ coupling constants were then computed according to the above-described four-step procedure. Structural results for this simulation are described first, and NMR coupling constants are given afterwards.

CP simulation results: The behavior of the three dimethyl ether molecules coordinated to Li is illustrated in Figure 8, which plots the three Li···O distances as a function of simulation time. It appears that decoordination of one of the three Me_2O molecules occurs within 4 ps. The simulation was stopped after 6 ps because complete expulsion of this solvent species at distances larger than 6 Å took place and caused the simulation to diverge due to the size of the box chosen. Thus, the simulations were rerun in a larger box (16 Å single cell used initially was switched to a 20 Å cell coupled to a dual box of 30 Å). Similar decoordination was observed within a few picoseconds in all cases. The results from the latter simulation are the only ones reported here.

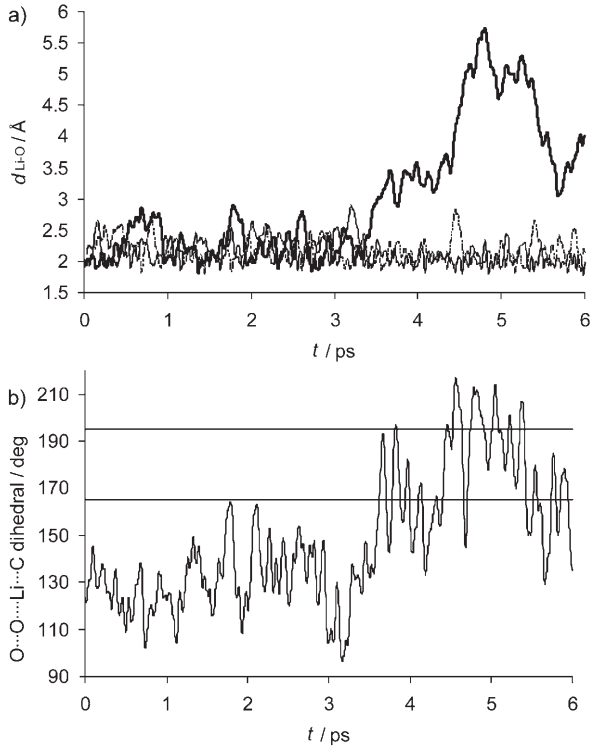

Figure 8. Li···O distances (a) and O-O-Li-C dihedral angle (b) as functions of time.

Using such a large box gives access to the behavior of the system during the period in which the ether molecule is partially decoordinated. For that time period, two different ranges are observed for the long Li···O distance which evolves at values of about 3.5 or about 5.5 Å. The differences between these two periods can be visualized by means of the snapshots of the structures in Figure 9. The central snapshot is a characteristic structure for Li···O at about 3.5 Å, whereas the right-hand one is characteristic of longer Li···O distances. This lengthening is linked to inversion of the pyramidalization at the Li atom. For short Li···O distances, Li^+ points toward the leaving ether (O-O-Li-C dihedral angle about 165°, Figure 5) whereas for long Li···O distances, it points in the opposite direction (O-O-Li-C dihedral angle about 195°). The connection between the Li···O bond length and the dihedral angle is easily seen by comparing Figure 8, top and bottom.

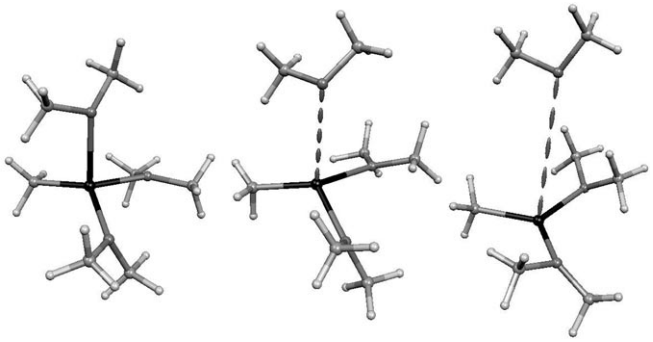

Figure 9. Snapshots of $MeLi(OMe_2)_3$ for $t=2.5$ (left), 4.0 (center), and 5.0 ps (right).

Static interpretation: Thermal decoordination of dimethyl ether can also be studied by a "static" approach. The free energy for the decoordination reaction [Eq. (5)]

$$MeLi(OMe_2)_3 \rightarrow MeLi(OMe_2)_2 + OMe_2 \quad (5)$$

can be evaluated by using statistical thermodynamics and the harmonic approximation for vibrational frequencies.[36] Correction for the basis set superposition error (BSSE) was considered and taken into account by means of the counterpoise method.[37] The results are gathered in Table 6. The reaction energy was found to be between $+5.0$ kcal mol^{-1} and

Table 6. Energetic data for the desolvation process computed at the BLYP/6-31++G** level.

ΔE [kcal mol^{-1}]	+5.0
$\Delta(E)$+BSSE [kcal mol^{-1}][a]	+3.6
$\Delta(E$+ZPE)+BSSE [kcal mol^{-1}]	+3.1
ΔS [cal mol^{-1} K^{-1}]	+31.9
ΔF+BSSE [kcal mol^{-1}]	−7.0

[a] MP2: 7.8 kcal mol^{-1}; HF: 5.0 kcal mol^{-1}; B3P86: 5.5 kcal mol^{-1}; B3LYP: 5.1 kcal mol^{-1}; B3PW91: 4.1 kcal mol^{-1}; PBE1PBE: 6.7 kcal mol^{-1}.

Table 7. Static and 300 K averaged (RMSDs in parentheses) for the Li–C, Li–O distances and $^1J_{Li,C}$ in $CH_3Li(Me_2O)_n$ (see text for details). Geometries were optimized at the BLYP/6–31++G** level. $^1J_{Li,C}$ were computed at the BLYP/6-311+G** level.

	Unsolvated	Static ($3OMe_2$)	Static ($2OMe_2$)	Whole simulation	Dynamic ($3OMe_2$)	Dynamic ($2+1OMe_2$)
Li–C [Å]	1.99 (0.07)	2.10	2.05	2.09 (0.09)	2.11 (0.10)	2.06 (0.08)
Li–O [Å]	–	2.08	1.96	2.14 (0.19)	2.21 (0.20)	2.05 (0.12)
			2.03	2.18 (0.19)	2.20 (0.19)	2.14 (0.20)
				3.02 (1.06)	2.26 (0.26)	4.07 (0.83)
$^1J_{Li,C}$ [Hz]	40.61 (2.70)	18.76	22.42	21.05 (3.04)	19.83 (2.67)	22.75 (2.73)

+3.3 kcal mol^{-1}, depending on the corrections taken into account. The energetics are thus slightly in favor of solvent coordination. Nevertheless, the dissociative character of this reaction suggests it should be entropically favored. In fact, ΔS was evaluated as 31.9 cal mol^{-1} K^{-1}, which results in a contribution to the free energy of −9.5 kcal mol^{-1} at 298 K. This value is in line with some experimentally and theoretically available data for various dissociative processes,[38] including those obtained for a closely related lithium enolate model.[39] The resulting free enthalpy for the reaction is thus negative, that is, static quantum results can account for the observed decoordination process. A similar result is expected with other computational levels or functionals: the largest ΔE+BSSE value is 7.8 kcal mol^{-1} (MP2 level), which is significantly smaller than the entropic contribution (−9.5 kcal mol^{-1}) responsible for solvent decoordination. This evidences the difficulty associated with choosing the degree of discrete solvation for the static evaluation of NMR constants from optimized structures, since reasoning relying on pure free energy only suggests a disolvated structure. Nevertheless, it is worth noting that such a computation does not take the solvent bulk into account, the effects of which cannot be simply predicted from phenomenological considerations.

Geometrical and NMR statistical properties: For statistical purposes, the overall simulation was split into a trisolvated part ($t<3$ ps) and a disolvated one ($t>4$ ps). None of these simulation lengths can be considered long enough for high-quality sampling, but they can help to evaluate the effect of explicit solvation on Li. The averaged values for the whole simulation are also reported (Table 7). The averaged and static Li–C distances are similar (within 0.01 Å) in both the tri- and the disolvated cases. The RMSDs are similar for both the di- and the trisolvated systems: solvation hardly affects the Li–C bond length and its floppiness. In contrast, the Li···O distances seem much more sensitive to thermal effects. Indeed, the average Li···O distances are significantly longer than their static analogues.

Unlike the Li–C distance, the $^1J_{Li,C}$ value is significantly affected by thermal effects. For the trisolvated part of the simulation, it is larger (19.8 Hz) than the static value (18.8 Hz). This thermal increase in $^1J_{Li,C}$ is also observed for the disolvated species, but to a much smaller extent (22.8 vs 22.4 Hz). Again, all RMSDs are similar and are comparable to those of the unsolvated species.

Even though accounting for explicit solvation is essential to accurately evaluate NMR coupling constants and can be carried out by using a static approach, the above results show that considering simultaneously the dynamic character of solvent coordination can significantly modify the obtained $^1J_{Li,C}$. As the representation of the sole first solvation shell in vacuum is not sufficient to fully account for the complexity of solvation, the modeling of bulk effects by periodic or spherical boundary conditions has been tested in a large number of systems involving water as solvent.[40] In our case, since ethereal solvents are concerned, such studies most probably require use of molecular mechanics (MM), either as such[41] or as part of a mixed quantum mechanics (QM)/MM scheme[42] in order to deal with the intrinsically large size of the experimental systems. This conclusion is buttressed by the fact that dimethyl ether is not a sufficient model for diethyl ether.[19] Hopefully, using a complete representation of the solvent will allow fine effects to be accounted for. Let us mention, for example, the differences observed in reactivity and spectroscopy when switching from THF to diethyl ether.[43]

Conclusions

Taking thermal effects into account is essential when dealing with the energetics of associative/dissociative reactions. Little is known about the influence of such effects on NMR coupling constants. A protocol is proposed and validated to compute such values from Car–Parrinello simulations. It was applied to evaluate the consequences of taking the dynamic behavior of aggregated and solvated MeLi species into account when dealing with the $^1J_{Li,C}$ coupling constants. The results show that a dispersion of about 2 Hz is associated with this parameter, whatever the intrinsic value of the constant. The time-averaged $^1J_{Li,C}$ is hardly different from that obtained from static quantum chemical computations. However, a detailed analysis shows that the CP simulations offer access to the chemically relevant parameters governing the coupling constant and thus open what remains otherwise a global black box. This part of the study suggests that thermal fluctuations can generally be neglected, except when large-amplitude motions such as conformational equilibrium or dynamic solvent decoordination are taken into account. In all cases, it is of prime importance to properly reproduce the experimental systems: whatever the species investigated here, the $^1J_{Li,C}$ coupling constants were shown to be much more sensitive to the degree of aggregation and number of solvent molecules in the first solvation shell than to thermal motions. Consequently, a proper definition of the system sampled, when not available from experimental data, should be considered first. Then, applying the proposed protocol

seems appropriate to examine the effects of temperature or those of structural flexibility as well as the role of the solvent. Selected examples of other organolithium aggregates of experimental interest are currently under study.

Acknowledgements

Calculations were performed on supercomputers at CRIHAN (Saint-Etienne-du-Rouvray, France), CINES (Montpellier, France), IDRIS (Orsay, France), and CCRE (Université Paris VI, France). We wish to acknowledge Dr. L.-H. Jolly (LCT, Paris, France) for technical support.

[1] a) B. J. Wakefield, *The Chemistry of Organolithium Compounds*, Pergamon Press, Oxford, **1974**; b) J. Clayden, *Organolithium: Selectivity for Synthesis*, Pergamon Press, Oxford, **2002**.
[2] J. F. McGarrity, C. A. Ogle, Z. Brich, H. R. Loosli, *J. Am. Chem. Soc.* **1985**, *107*, 1810.
[3] A. Johansson, A. Pettersson, Ö. Davidsson, *J. Organomet. Chem.* **2000**, *608*, 153.
[4] a) B. Qu, D. B. Collum, *J. Am. Chem. Soc.* **2005**, *127*, 10820; b) S. J. Zuend, A. Ramirez, E. Lobkovsky, D. B. Collum, *J. Am. Chem. Soc.* **2006**, *128*, 5939.
[5] a) A. Streitwieser, E. Juaristi, Y.-J. Kim, J. K. Pugh, *Org. Lett.* **2000**, *2*, 3739; b) Y.-J. Kim, A. Streitwieser, *Org. Lett.* **2000**, *2*, 573.
[6] D. R. Armstrong, S. C. Ball, D. Barr, W. Clegg, D. J. Linton, L. C. Kerr, D. Moncrieff, P. R. Raithby, R. J. Singer, R. Snaith, D. Stalke, A. E. H. Wheatley, D. S. Wright, *J. Chem. Soc. Dalton Trans.* **2002**, 2505.
[7] W. Bauer, P. von R. Schleyer, *Adv. Carbanion Chem.* **1992**, *1*, 89, and references therein.
[8] H. Günther, *J. Braz. Chem. Soc.* **1999**, *10*, 241.
[9] A. Bagno, F. Rastrelli, G. Saielli, *Prog. Nucl. Magn. Reson. Spectrosc.* **2005**, *47*, 41.
[10] W. Bauer, W. R. Winchester, P. von R. Schleyer, *Organometallics* **1987**, *6*, 2371.
[11] O. Parisel, C. Fressigné, J. Maddaluno, C. Giessner-Prettre, *J. Org. Chem.* **2003**, *68*, 1290.
[12] a) T. Koizumi, O. Kikuchi, *Organometallics* **1995**, *14*, 987; b) T. Koizumi, K. Morohashi, O. Kikuchi, *Bull. Chem. Soc. Jpn.* **1996**, *69*, 305.
[13] H. Gérard, A. de la Lande, J. Maddaluno, O. Parisel, M. E. Tuckerman, *J. Phys. Chem. A* **2006**, *110*, 4787.
[14] a) J. Schmidt, D. Sebastiani, *J. Chem. Phys.* **2005**, *123*, 074501; b) S. Rossano, F. Mauri, C. J. Pickard, I Farnan, *J. Phys. Chem. B* **2005**, *109*, 7245.
[15] See among others: a) M. Bühl, M. Parrinello, *Chem. Eur. J.* **2001**, *7*, 4487; b) D. Sebastiani, M. Parrinello, *ChemPhysChem* **2002**, *3*, 675; c) T. C. Ramalho, M. Bühl, *Magn. Reson. Chem.* **2005**, *43*, 139; d) M. Bühl, S. Grigoleit, *Organometallics* **2005**, *24*, 1516; e) M. Bühl, *J. Phys. Chem. A* **2002**, *106*, 10505; f) C. Raynaud, L. Maron, J.-P. Daudey, F. Jolibois, *ChemPhysChem* **2006**, *7*, 407; g) M. Pavone, V. Barone, I. Ciofini, C. Adamo, *J. Chem. Phys.* **2004**, *120*, 9167; h) O. Crescenzi, M. Pavone, F. De Angelis, V. Barone, *J. Phys. Chem. B* **2005**, *109*, 445; i) O. V. Yazyev, L. Helm, *Theor. Chem. Acc.* **2006**, *115*, 190.
[16] a) J. Vaara, J. Lounila, K. Ruud, T. Helgaker, *J. Chem. Phys.* **1998**, *109*, 8388; b) Y. Ellinger, F. Pauzat, V. Barone, J. Douady, R. Subra, *J. Chem. Phys.* **1980**, *72*, 6390; c) F. Pauzat, H. Gritli, Y. Ellinger, R. Subra, *J. Phys. Chem.* **1984**, *88*, 4581.
[17] F. E. Romersberg, D. B. Collum, *J. Am. Chem. Soc.* **1994**, *116*, 9187.
[18] F. E. Romersberg, D. B. Collum, *J. Am. Chem. Soc.* **1994**, *116*, 9198.
[19] L. M. Pratt, *Bull. Chem. Soc. Jpn.* **2005**, *78*, 890.
[20] R. Car, M. Parrinello, *Phys. Rev. Lett.* **1985**, *55*, 2471.
[21] a) T. Helgaker, M. Jaszuñski, K. Ruud, *Chem. Rev.* **1999**, *99*, 293; b) J. Vaara, J. Jokisaari, R. E. Wasylischen, D. L. Bryce, *Prog. Nucl. Magn. Reson. Spectrosc.* **2002**, *41*, 233; c) M. Bühl, M. Kaupp, O. L. Malkina, V. G. Malkin, *J. Comput. Chem.* **1999**, *20*, 91.
[22] Gaussian 03, Revision A.1, M. J. Frisch, G. W. Trucks, H. B. Schlegel, G. E. Scuseria, M. A. Robb, J. R. Cheeseman, J. A. Montgomery, Jr., T. Vreven, K. N. Kudin, J. C. Burant, J. M. Millam, S. S. Iyengar, J. Tomasi, V. Barone, B. Mennucci, M. Cossi, G. Scalmani, N. Rega, G. A. Petersson, H. Nakatsuji, M. Hada, M. Ehara, K. Toyota, R. Fukuda, J. Hasegawa, M. Ishida, T. Nakajima, Y. Honda, O. Kitao, H. Nakai, M. Klene, X. Li, J. E. Knox, H. P. Hratchian, J. B. Cross, C. Adamo, J. Jaramillo, R. Gomperts, R. E. Stratmann, O. Yazyev, A. J. Austin, R. Cammi, C. Pomelli, J. W. Ochterski, P. Y. Ayala, K. Morokuma, G. A. Voth, P. Salvador, J. J. Dannenberg, V. G. Zakrzewski, S. Dapprich, A. D. Daniels, M. C. Strain, O. Farkas, D. K. Malick, A. D. Rabuck, K. Raghavachari, J. B. Foresman, J. V. Ortiz, Q. Cui, A. G. Baboul, S. Clifford, J. Cioslowski, B. B. Stefanov, G. Liu, A. Liashenko, P. Piskorz, I. Komaromi, R. L. Martin, D. J. Fox, T. Keith, M. A. Al-Laham, C. Y. Peng, A. Nanayakkara, M. Challacombe, P. M. W. Gill, B. Johnson, W. Chen, M. W. Wong, C. Gonzalez, J. A. Pople, Gaussian, Inc., Pittsburgh, PA, **2003**.
[23] M. E. Tuckerman, D. A. Yarne, S. O. Samuelson, A. L. Hughes, G. J. Martyna, *Comput. Phys. Commun.* **2000**, *128*, 333.
[24] a) A. D. Becke, *Phys. Rev.* **1988**, *A38*, 2155; b) A. D. Becke, *J. Chem. Phys.* **1992**, *96*, 2155; c) C. Lee, W. Yang, R. C. Parr, *Phys. Rev. B* **1988**, *37*, 785.
[25] C. Hartwigsen, S. Goedecker, J. Hutter, *Phys. Rev. B* **1998**, *58*, 3641.
[26] N. Troullier, L. Martins, *Phys. Rev. B* **1991**, *43*, 1993.
[27] G. J. Martyna, M. E. Tuckerman, *J. Chem. Phys.* **1999**, *110*, 2810.
[28] D. A. Yarne, M. E. Tuckerman, G. J. Martyna, *J. Chem. Phys.* **2001**, *115*, 3531.
[29] G. J. Martyna, M. E. Tuckerman, M. L. Klein, *J. Chem. Phys.* **1992**, *97*, 2635.
[30] a) J. P. Perdew, *Phys. Rev. B* **1986**, *33*, 8822; b) A. D. Becke, *J. Chem. Phys.* **1993**, *98*, 5648.
[31] a) J. P. Perdew, K. Burke, M. Ernzerhof, *Phys. Rev. Lett.* **1996**, *77*, 3865; b) J. P. Perdew, K. Burke, M. Ernzerhof, *Phys. Rev. Lett.* **1997**, *78*, 1396.
[32] a) M. Karplus, *J. Chem. Phys.* **1959**, *30*, 11; b) R. H. Contreras, J. E. Peralta, *Prog. Nucl. Magn. Reson. Spectrosc.* **2000**, *36*, 321.
[33] See, for example: J. A. Pople, W. G. Schneider, H. J. Bernstein, *High-resolution Nuclear Magnetic Resonance*, McGraw-Hill, New-York, **1959**.
[34] K. Ruud, T. Helgaker, P. Jørgensen, K. L. Bak, *Chem. Phys. Lett.* **1994**, *226*, 1.
[35] W. Bauer, C. Griesinger, *J. Am. Chem. Soc.* **1993**, *115*, 10871.
[36] D. A. McQuarrie, J. D. Simon, *Molecular Thermodynamics*, University Science Books, Sausalito, **1999**.
[37] a) P. Hobza, R. Zahradnik, *Chem. Rev.* **1988**, *88*, 871; b) F. Boys, F. Bernardi, *Mol. Phys.* **1970**, *19*, 553.
[38] a) J. A. Campbell, *J. Chem. Educ.* **1985**, *62*, 231; b) M. E. Mina da Piedade, J. A. Martinho Simões, *J. Organomet. Chem.* **1996**, *518*, 167; c) L. A. Watson, O. Eisenstein, *J. Chem. Educ.* **2002**, *79*, 1269.
[39] A. Abbotto, A. Streitwieser, P. von R. Schleyer, *J. Am. Chem. Soc.* **1997**, *119*, 11255.
[40] For Li^+: a) S. Izvekov, M. R. Philpott, *J. Chem. Phys.* **2000**, *113*, 10676; b) S. B. Rempe, L. R. Pratt, G. Hummer, J. D. Kress, R. L. Martin, A. Redondo, *J. Am. Chem. Soc.* **2000**, *122*, 966; c) A. P. Lyubartsev, K. Laasonen, A. Laaksonen, *J. Chem. Phys.* **2001**, *114*, 3120.
[41] a) H. H. Loeffler, *J. Comput. Chem.* **2003**, *24*, 1232; b) D. Spångberg, R. Rey, J. T. Hynes, K. Hermansson, *J. Phys. Chem. B* **2003**, *107*, 4470; c) S. Chowdhuri, A. Chandra, *J. Chem. Phys.* **2003**, *118*, 9719; d) A. V. Egorov, A. V. Kommolkin, P. V. Yushmanov, A. P. Lyubartsev, A. Laaksonen, *J. Phys. Chem. B* **2003**, *107*, 3234.
[42] a) A. Tongraar, K. R. Liedl, B. M. Rode, *Chem. Phys. Lett.* **1998**, *286*, 56; b) H. H. Loeffler, A. M. Mohammed, Y. Inada, S. Funahashi, *Chem. Phys. Lett.* **2003**, *379*, 452.
[43] See for instance: a) B. L. Lucht, D. A. Collum, *J. Am. Chem. Soc.* **1994**, *116*, 6009; b) B. L. Lucht, D. A. Collum, *J. Am. Chem. Soc.* **1995**, *117*, 9863; c) P. I. Arvidsson, Ö. Davidsson, *Angew. Chem.* **2000**, *112*, 1527; *Angew. Chem. Int. Ed.* **2000**, *39*, 1467; d) P. I. Ar-

vidsson, Ö. Davidsson, *Angew. Chem.* **2000**, *112*, 1527; e) G. Hilmersson, *Chem. Eur. J.* **2000**, *6*, 3069; f) R. Sott, J. Granander, G. Hilmersson, *Chem. Eur. J.* **2002**, *8*, 2081; g) J. Granander, R. Sott, G. Hilmersson, *Chem. Eur. J.* **2006**, *12*, 4191; h) Y. Yuan, S. Desjardins, A. Harrison-Marchand, H. Oulyadi, C. Fressigné, C. Giessner-Prettre, J. Maddaluno, *Tetrahedron* **2005**, *61*, 3325.

Received: July 31, 2006
Revised: October 3, 2006
Published online: January 16, 2007

